

Article

Simulation Study on Nitrogen Pollution in Shallow Groundwater in Small Agricultural Watersheds in the Huixian Wetland

Zupeng Wan ^{1,2}, Junfeng Dai ^{2,3,*}, Linyan Pan ⁴ , Junlei Han ¹, Zhangnan Li ¹ and Kun Dong ^{1,2} ¹ College of Environmental Science and Engineering, Guilin University of Technology, Guilin 541004, China² Guangxi Key Laboratory of Environmental Pollution Control Theory and Technology, Guilin University of Technology, Guilin 541004, China³ Collaborative Innovation Center for Water Pollution Control and Water Security in Karst Region, Guilin University of Technology, Guilin 541004, China⁴ College of Environment and Resources, Guangxi Normal University, Guilin 541004, China

* Correspondence: whudjf@163.com

Abstract: In this study, we investigated the influence of different simulations on the transport of shallow groundwater nitrogen in the Mudong River watershed of the Huixian Wetland, a karst wetland. Based on GMS (Groundwater Modeling System) software, the equivalent porous media model was used to simulate the transport of total nitrogen under different conditions in the study area. Two years of field monitoring data in the study area provided the input for the modeling. The SWAT (soil and water assessment tool) model was used to divide the study area into sub-basins. The initial concentration flux index *W* is first introduced in the equivalent porous medium model to calculate the initial concentration. The simulation results showed the difference between the simulated and monitored values of total nitrogen concentration was between 20% and 40% in 22.2% of the cases, and less than 20% in 66.7% of the cases, indicating that the solute transport model has good applicability in the Huixian Wetland. Parameter sensitivity analysis showed that fertilizer application was the main factor influencing total nitrogen. A 25% reduction in fertilizer application reduced total nitrogen emissions by 31.5% in sub-basin S3 and 22.5% in sub-basin S4. These reductions were greater than the abatement effect of changing land cover and managing river pollution. The pollution plume of total nitrogen was reduced by 38.5% in the southern part of sub-basin S3 (Mudong Lake) and by 40.2% in the western part of sub-basin S4 (Blacksmithing Village). The average concentration was reduced by 2.04 mg/L and 1.22 mg/L, respectively. This study shows that reasonable control of double-season rice nitrogen fertilizer application and appropriate land cover modification can help reduce total nitrogen emissions from wetlands in the Li River watershed and ensure the sustainable development of the local economy and groundwater.



Citation: Wan, Z.; Dai, J.; Pan, L.; Han, J.; Li, Z.; Dong, K. Simulation Study on Nitrogen Pollution in Shallow Groundwater in Small Agricultural Watersheds in the Huixian Wetland. *Water* **2022**, *14*, 3657. <https://doi.org/10.3390/w14223657>

Academic Editors: Xiaohu Wen, Yifeng Wu, Changwen Ma and Jun Wu

Received: 6 October 2022

Accepted: 11 November 2022

Published: 13 November 2022

Publisher's Note: MDPI stays neutral with regard to jurisdictional claims in published maps and institutional affiliations.



Copyright: © 2022 by the authors. Licensee MDPI, Basel, Switzerland. This article is an open access article distributed under the terms and conditions of the Creative Commons Attribution (CC BY) license (<https://creativecommons.org/licenses/by/4.0/>).

Keywords: non-point source pollution; total nitrogen; GMS model; karst wetland

1. Introduction

A good understanding of contaminant transport characteristics in the subsurface environment is a prerequisite for sustainable groundwater use and management [1]. Agricultural surface source pollution infiltration is a significant cause of groundwater contaminants exceeding prescribed limits. Studies have found that the vast majority of pollution is discharged in small areas [2–4]. However, the sources of pollution in residential areas are complex and widely distributed, making it difficult to achieve targeted treatment [5]. Therefore, identifying and assessing high-pollution risk areas and high-pollution output periods is essential for efficient pollution management.

When researching groundwater nitrogen pollution due to agricultural surface pollution, investigating the pollution source is a critical and complex problem. Under the

condition of knowing the spatial and temporal distribution of the contamination plume, groundwater contamination source parameters are generally calculated using the inverse method, for example, to find the contaminant leakage intensity. Newman first used the inversion method for hydrology and divided the inversion method into direct and indirect methods. Some researchers have used the Bayesian formulation [6], Kalman filtering method [7,8], and multi-chain MCMC algorithm [9,10] for inversion.

There are few cases of generalized groundwater transport simulation based on sub-basin zoning. In this study, the SWAT model was used to divide the study area into sub-basins (catchment areas) to reduce the non-adaptability of the inverse problem solution. The priority source area of the pollutants for the MT3DMS module of the GMS model was defined based on the discharge load status of the sub-basins. The initial concentration flux W was used with the simulated surface and subsurface monitoring point data to calculate and invert the initial concentration of the pollutant sources in each sub-basin.

Karst aquifers are highly inhomogeneous, containing many large fissures and underground pipes, so they are usually more vulnerable to pollution than non-karst areas [11]. The Huixian Wetland in Lingui District, Guilin, Guangxi is the largest pristine karst wetland in the Li River basin. Within the Mudong River watershed of the Huixian Wetland, the high rate of fertilizer application (298.8 kg/hm^2), high ratio of nitrogen in the fertilizer, the application ratio of nitrogen, phosphorus, and potassium is 1:0.34:0.28 [12]. The inadequate treatment of runoff from aquatic and livestock farms (only 40% harmless treatment) has created a serious pollution problem. The karst geomorphic features drive the hydraulic transport process of pollutants in the groundwater system. Scientists have explored the correlation between nitrogen and phosphorus pollutant indicators in the Huixian Wetland and studied the eutrophication and ecological degradation of the wetland [13]. Zhi-Li Ren [14] simulated groundwater levels in the Huixian Wetland, but there is a lack of research on the effects of surface source pollution on nitrogen transport in shallow groundwater in the Huixian Wetland. In this paper, we analyze the effects of different pollution control scenarios on solute transport in shallow groundwater, and then design a Class II water concentration standard that meets the Groundwater Quality Standard (GB/T 14848-2017) (hereafter referred to as the standard). This standard will support the prevention and control of nitrogen pollution in groundwater in the Huixian Wetland.

2. Materials and Methods

2.1. Study Area

The study area was the Mudong River watershed of the Huixian Wetland in the Li River basin (Figure 1). After the field survey, the Mudong River watershed has a fixed head boundary and a fixed flow boundary for which the source and sink can be calculated. The water balance is in a positive equilibrium state, which is typical for a karst-closed sub-basin. The rainfall is abundant and concentrated in April–September. The average annual temperature is $21 \text{ }^\circ\text{C}$. The longest dimension is from east to west (7.71 km), the width from north to south is 8.36 km, and the area is about 31.09 km^2 .

Groundwater in the Mudong River watershed flows from north to south. In the Mudong drainage area, groundwater as a whole flow from northeast to southwest, discharging into the Mudong River (Figure 2). The water-bearing system in the Mudong River watershed consists of a Quaternary loose rock group and a Devonian and Carboniferous carbonate rock group. The carbonate rocks can be divided into continuous pure carbonate rocks and interlayer impure carbonate rocks [15]. The groundwater types in the Mudong River watershed are carbonate karst water and Quaternary pore water. The Quaternary pore water occurs in the Quaternary sediments with a thickness of about 0.2–6 m in the center of the wetland.

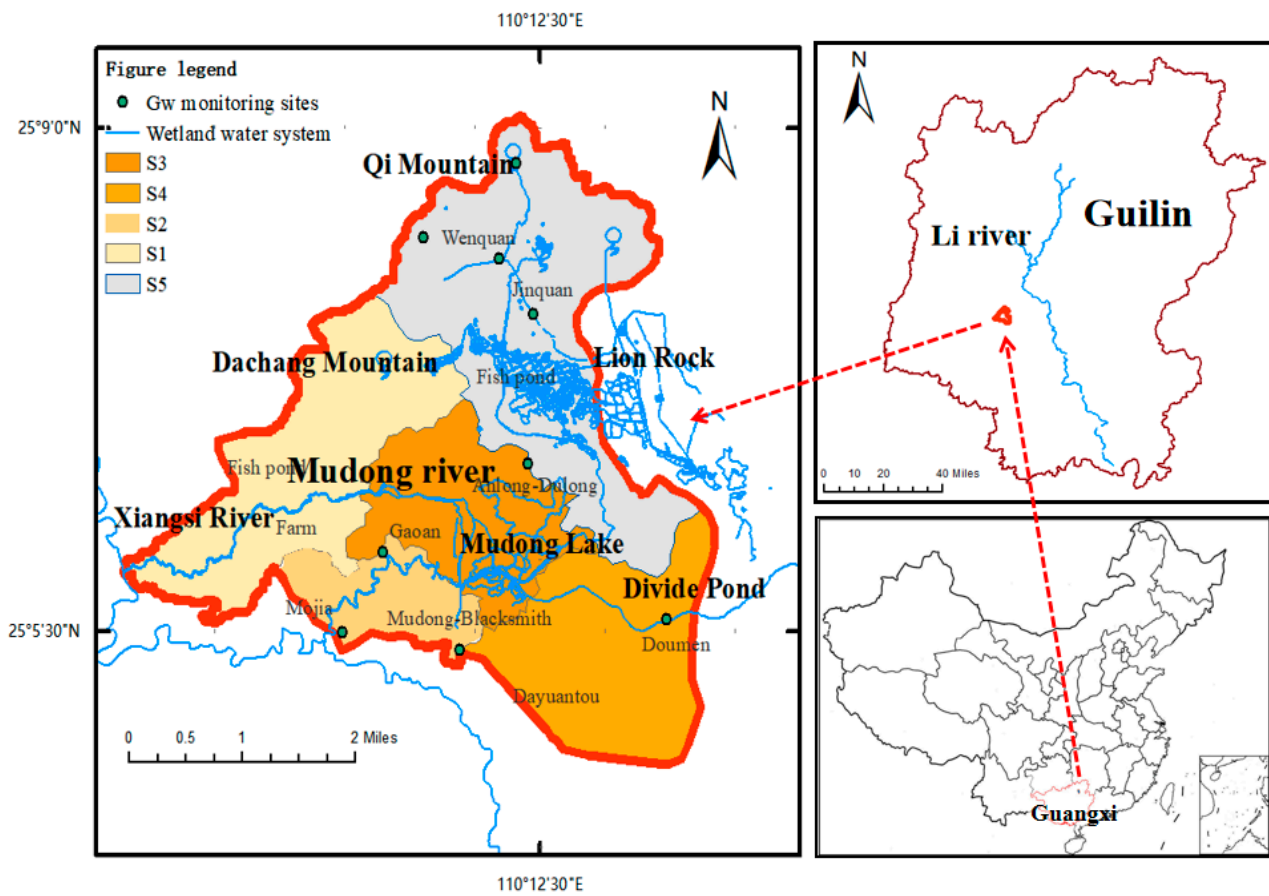


Figure 1. Distribution of sub-basins in the study area.

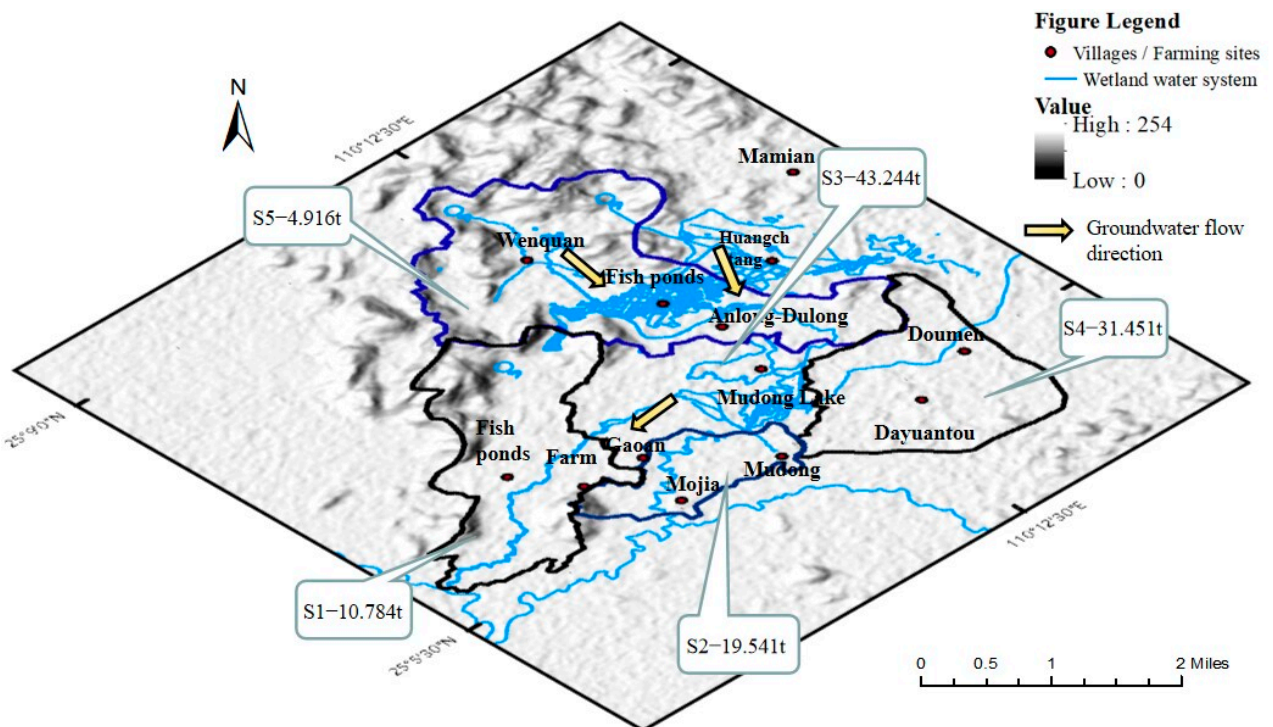


Figure 2. The spatial distribution of monthly average total nitrogen load in the study area in 2019 (unit: ton).

2.2. Establishment of Conceptual Model

A 3D visualization Groundwater Modeling System (GMS) was used in the research. The fissures and karst water flows in the Mudong River watershed migrate in a zigzagging network of fissures and karst caves. Based on the equivalent porous medium method, this paper approximates the equivalent porous medium from the macro level. The anisotropic flow characteristics under dominant control are generalized. The mathematical model of solute transport was as follows:

$$-\frac{\partial}{\partial x_i}(v_i C) + \frac{\partial}{\partial x_i} \left(D_{ij} \frac{\partial C}{\partial x_j} \right) - \lambda \left(C + \rho_b \frac{S}{\theta} \right) \pm \frac{q_s}{\theta} C_s = R \frac{\partial C}{\partial t} \quad (1)$$

In Equation (1), V_i : actual permeate flow rate (m/d); D_{ij} : dispersion coefficient component (m^2/d); S : adsorption term concentration (kg/kg); C_s : source-sink term concentration (kg/m^3); θ : effective porosity (dimensionless). R : retardation factor (dimensionless); and ρ_b : bulk density (kg/m^3).

Because the migration mechanism of groundwater pollutants is more focused on the structure and characteristics of the hydrostratum, the stratigraphic structure is further simplified to make it more consistent with the hydrogeological characteristics based on analyzing and studying the regional geological structure and geological conditions. Considering that this study focuses on analyzing shallow groundwater pollution and migration, the grid is divided into an Unconfined aquifer. Based on the collected data and calculation results of hydrogeological parameters, a three-dimensional hydrogeological conceptual model of the small agricultural watershed of Mudong River was constructed, and a mathematical model of the three-dimensional stable flow of heterogeneous and isotropic and the boundary conditions were established. According to the theory of groundwater dynamics, the boundary conditions were as follows: the surface water watershed composed of Dachang Mountain, Flag Mountain and Lion Rock in the northern part of the Mudong River watershed forms the second type of water separation boundary, and the surface water watershed in the southeast is used as the second type of zero flow boundary. The Mudong River flows westward into the Xiangsi River section as the first type of fixed head boundary. The groundwater discharges from the north and south to the central Mudong River.

We imported coordinate elevation data into the GMS, established the conceptual model (boundary, source sink, parameter partition, common module), and created a 3D grid according to the conceptual model. The conceptual model with the MODFLOW computational model was matched, assigned hydrogeological parameters, and the MT3DMS solute transport model was established. On the basis of considering the monitoring points of surface water and groundwater, the river network data of the watershed of Mudong River was digitized through the Omap interactive map. Using ArcGIS software, SWAT model, digital elevation model (DEM) data and river network data, the small watershed of Mudong River was divided, the Mudong River watershed is divided into five sub-basins, and the details of the sub-basins are shown in Figure 1 and Table 1.

The most common way to delineate high pollution risk areas is to calculate the loadings of each sub-basin (based on the pollution discharge loadings of each sub-basin outlet monitoring cross-section) and then apply ArcGIS software to analyze the spatial distribution of the total nitrogen pollution discharge loadings in the Mudong River watershed. Since water quality prediction and basin surface source pollution control planning requires annual loadings under different conditions, the basin outlet cross-section (or other control section) total annual load (W_t) can be expressed as:

$$W_t = C_{SM} \int_{t_0}^{t_e} Q_s(t) dt + C_{BM} \int_{t_0}^{t_e} Q_B(t) dt = C_{SM} W_s + C_{BM} W_B \quad (2)$$

In Equation (2), C_{SM} and C_{BM} are the average concentrations of nitrogen and phosphorus in surface runoff and subsurface runoff, respectively; Q_s is the surface water runoff

flow, Q_B is the underground river runoff flow; t_n is the monitoring time in January, t_e is the monitoring time in December; W_S and W_B are the total annual surface and subsurface runoff, respectively. The average monthly load in the sub-basin of Mudong River watershed is calculated as follows.

$$L = \frac{[(C \times Q) \times 10^{-3} \times T]}{S} \quad (3)$$

In Equation (3), L is the nitrogen and phosphorus discharge load (kg/km²); C is the mass concentration of nitrogen and phosphorus in runoff discharge at each scale (mg/L); Q is the river runoff flow at the monitoring point (m³/s); S is the control area of the sub-basin (km²); T is the time of the month in seconds (s).

Table 1. Overview of the sub-basins in the study area.

Sub-Basin Number	Area (km ²)	Sub-basin Outlets	Sub-basin Water System	Crop	Soil Type/Material	kv (cm/s)
s1	6.0625	Mudong River Outfall	Downstream section of Mudong River	Rice	Red soil/rice soil	1.8×10^{-5}
s2	3.2333	Agricultural branch canals	Ancient Guilieu Canal	Rice, oranges	Red soil/construction land	1.2×10^{-6}
s3	4.9433	Middle Mudong River	Middle section of Mudong River, Mudong Lake	Rice, oranges	Red and yellow soil/swampy soil	0.8×10^{-6}
s4	6.8087	Sanyi Pier	Ancient Guilieu Canal, Fenshui Pond	Rice	Red soil/rice soil	0.9×10^{-6}
s5	9.9488	Mamian Branch Canal	Upstream section of Mudong River, Dulongtang	Rice, corn, and watermelon	Limestone soils/swampy soils, rice soils	0.71×10^{-6}

The average concentration of total phosphorus in the shallow groundwater of the Mudong River watershed was 0.07 mg/L. The migration process was extremely insignificant in months with low rainfall. Nitrogen pollution from agricultural fields has become one of the most important sources of pollution in agricultural environments [16]. Nitrogen pollutants are easily adsorbed by particulate matter (sediment or colloid), which can reflect the effect of fertilization in the watershed. Therefore, the larger average concentration of total nitrogen (7.69 mg/L) was used as the transport component. The calculations showed that the monthly average emissions of total nitrogen pollution load in the S3 and S4 sub-basins in 2019 were 43.244 t and 31.451 t, respectively (Figure 2). Our preliminary finding is that the S3 and S4 sub-basins are high pollution risk areas for nitrogen pollution in the Mudong River watershed, contributing 67.94% of the total nitrogen pollution in the Mudong River watershed.

According to the analysis of pollutant source intensity, TN pollutants caused by surface source pollution were injected in an unsteady flow. We used the initial concentration flux index (W) to facilitate the calculation. We not only reflect the surface water pollution status but also can be combined with the permeability coefficient concentrations of different subsurface surfaces to determine hydrogeological status. Both surface water and groundwater pollute the total groundwater nitrogen concentration in this study, and the study uses the method of calculating the initial concentration flux W to analyze the effect of dual sources of pollution on the initial concentration of the model. The total nitrogen concentration of surface water was sampled in the river and measured by a flow injection analyzer. The infiltration coefficient was based on the infiltration model proposed by Green-Ampere and obtained using a double-loop infiltration test. The PEST module was used for reverse simulation; the parameters were fine-tuned according to its results. The

initial concentration flux checking coefficient is introduced to check the calculation results. The initial concentration calculation formula is:

$$W = \sum_{i=1}^n C_i Q_i \alpha_i K \times 8.35 \times 10^{-2} \quad (4)$$

In Equation (4), W is the initial concentration flux index of surface source pollution; i is the model time step; C_i is the surface water quality concentration, mg/L; Q is the current section of the Mudong River flow, m³/s; α_i is the initial concentration flux calibration coefficient; K is the infiltration coefficient.

The initial concentration calibration coefficient was calculated as:

$$\alpha = \frac{C_J Q_J}{C_S Q_S} \quad (5)$$

In Equation (5): α is the initial concentration flux calibration coefficient; C_J is the measured concentration at the monitoring point of Mudong River section, mg/L; Q_J is the calculated flow at the section, m³/s; C_S is the simulated concentration at the monitoring point of Mudong River section, mg/L; and Q_S is the simulated flow at the section, m³/s.

The initial concentration flux W obtained for each sub-basin was divided by the area of the sub-basin, and the model's initial concentration values were adjusted using the GMS identification model, as shown in Table 2.

Table 2. TN initial concentration setting.

Sub-Basins	Land Cover	Initial Concentration of Pollution Source (mg/L)
S1	Rice field (downstream of Mutong River)	11.0828
S4	Village District (Doumen)	21.2383
S2	Village District (Mudong)	18.8115
S3	Village District (Anlong)	26.2384
S5	Village District (Wenquan)	2.5124
-	Grassland Dryland	1.5414

2.3. GMS Model Validation

Using January 2020 to December 2020 as the validation phase of the model, the average water level and total nitrogen concentrations of the nine shallow groundwater monitoring wells are shown in Figure 3.

According to the Technical Specification for Groundwater Environmental Monitoring (HJT164-2020), the fitting error between the measured and simulated values at the monitoring point is no more than 1.2 m. Figure 3a shows that in the water level fitting process of the Mudong River watershed, the monitoring points whose difference between the simulated value and the measured value is less than 1.2 m meet the HJT164-2020 standard, and 80% of the monitoring points meet this standard. The statistical results of Figure 3b show that the error between the simulated value and measured value of total nitrogen is 44.4% within 10%, 22.2% within 10~20%, and 88.9% within 40%. There was no significant difference between the two t -test results with $p > 0.05$. In conclusion, the model has good applicability to the simulation of total nitrogen in the Mudong River watershed.

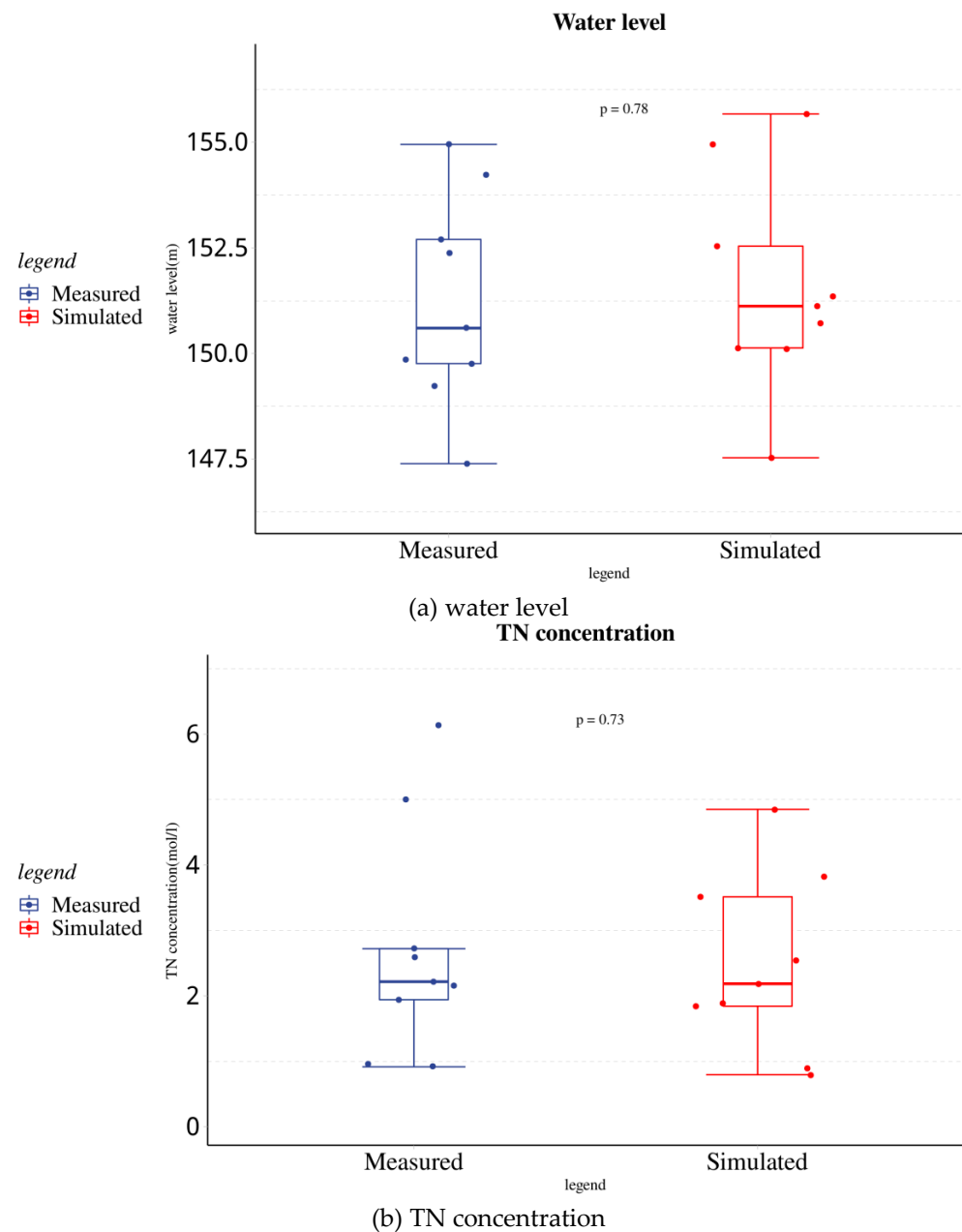


Figure 3. Error box simulation of the measured value error box plot. (a) water level, (b) TN concentration.

3. Simulation of Total Nitrogen Transport in Shallow Groundwater in Response to Different Management Measures

Different land cover types will lead to different surface source pollution output characteristics [17] and solute transport characteristics in groundwater. Fertilizer nutrient loss from rice fields and domestic runoff from villages and towns are the main sources of surface source pollution in the study area. Three scenarios were designed to simulate and analyze the effects of different management measures on the transport of total nitrogen in groundwater. For each scenario, the economy, population, and meteorology were assumed to be the same as the status quo year (2020).

3.1. Scenarios

Scenario 1: Reducing fertilizer application. According to the Guilin Statistical Yearbook, the amount of nitrogen and phosphorus fertilizer applied (calculated in pure terms)

to early and late rice in the Mudong River watershed in 2020 was about 411.01 kg/ha, and 59.41 kg/ha, including about 101.75 kg/ha and 15.85 kg/ha of basal fertilizer and about 153.15 kg/ha and 23.47 kg/ha for two follow-up fertilizers (urea:compound fertilizer = 4:6). Studies [18,19] have shown that after the fertilizer application reaches a certain level, additional fertilizer application does not increase yield and instead creates serious soil and water pollution. For Scenario 1, we assumed that the fertilizer application for early and late rice was reduced to 75% of the original amount.

Scenario 2: Changing the land cover. Heavy rainfall creates runoff containing dust and domestic waste from villages and townships. This runoff is a surface source of pollution. Hydrogeological surveys show that the vertical permeability coefficient (k) of soils in the villages and towns in the karst areas is $1 \times 10^{-4} \sim 1 \times 10^{-6}$ cm/s. In Scenario 2, we modeled an increase in the vegetation cover in villages and towns, the use of permeable roads, and a reduction in the impermeable area within the Mudong River watershed, resulting in an increase in k to 2.2×10^{-4} cm/s.

Scenario 3: Reducing pollutant concentrations in the Mudong River. The Mudong River was divided into six arc segments (2–3 km/segment) in the GMS. The pollutant concentration leached from the bottom of each arc segment of the envelope was set as the upper boundary condition of the saturated zone solute transport model. The concentration of each river section was adapted to the concentration of nearby village monitoring wells. In Scenario 3, we assumed that additional water quality treatment reduced the total nitrogen concentration in each river section module by 20% during the simulation period.

The specific scenario settings are shown in Table 3.

Table 3. Scenario setting of non-point source pollution control plan.

Scenario	Scenario Setting	Description	Model Implementation Method
Scenario 1	Reduce the amount of chemical fertilizers applied	Reduce fertilizer application by 75%	TN concentration in April and August in each sub-basin is 75% of the original
Scenario 2	Change land cover	Increase vegetation cover in village and town areas	Permeability coefficient of village area from $1 \times 10^{-4} \sim 1 \times 10^{-6}$ cm/s Increase to 2.2×10^{-4} cm/s
Scenario 3	Reduction of river solute concentration	River water quality management, reduce total nitrogen concentration in Mudong River	20% reduction in river module concentration

Shallow groundwater solute transport models were constructed based on the three scenarios. Sensitivity analysis was used to assess the effects of the scenarios on total nitrogen transport. This approach is based on the principle of using the model output results to find the bias of the input model scenario parameters and using the magnitude of the bias to determine the magnitude of the influence of the input model scenario parameters on the model output results (Equation (6), which can be rewritten as Equation (7) for the convenience of calculation).

$$S_i = \frac{\partial y}{\partial x_i} \tag{6}$$

$$S_k = \frac{\sum_{i=1}^n [y_i(x_k + \Delta x_k) - y_i x_k] \times y_i(x_k)^{-1}}{\Delta x_k \times (x_k)^{-1}} \tag{7}$$

In Equation (7), S_k is the sensitivity coefficient; x_k is the k th scenario parameter input to the model; Δx_k is the amount of change of the k th scenario parameter input to the model; $y_i(x_k + \Delta x_k)$ is the model output result when the scenario parameter changes Δx_k ;

$y_i(x_k)$ is the output result of the scenario parameter x_k time model; n is the number of monitoring wells in the study area. Avoiding measurements with high parameter correlations as much as possible may help ensure that the sensitivity matrix is well-conditioned [20,21]. The larger the sensitivity factor, the greater the effect of the scenario parameters on the solute model results.

3.2. Characteristics of Total Nitrogen Transport under Different Scenarios

The MT3DMS module was applied to solve the total groundwater nitrogen transport according to the three scenarios set in Table 3. The status quo year model M1 was calibrated to simulate a stress period from January 2020 to December 2020. Its simulation results for 123 d (fertilization at the tilling stage of early rice) and 245 d (fertilization at the end of late rice transplanting) are shown in Figure 4.

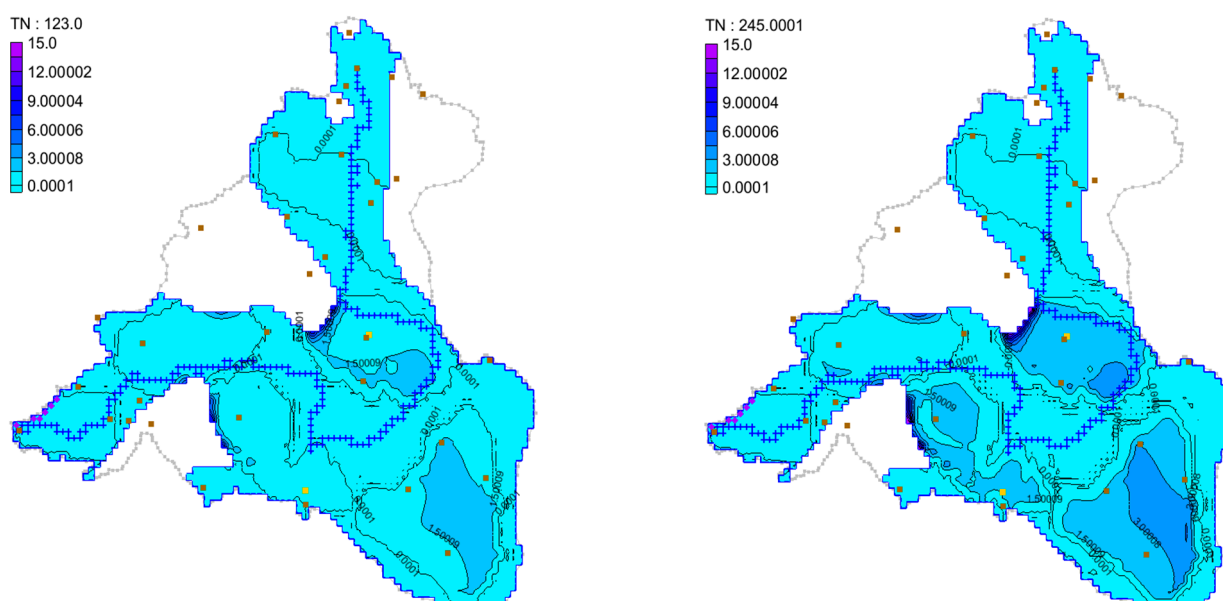


Figure 4. Total nitrogen simulation results at 123 d and 245 d of the current year model. Note: The blanks in the figure are karst solitary peaks/peak cluster depressions, and the aquifer is drained, so the model cannot display the simulation results.

The field investigation showed that 87.5% of the rice field area was in the S1, S3, and S4 sub-basins. Using the conventional urea nitrogen application, 25% of the nitrogen was saved in April–June (early rice transplanting and tilling fertilization) and August (late rice transplanting fertilization). Figure 5 shows the simulation results for 123 d and 245 d. The simulation results for 123 d and 245 d were adjusted from 12 m/d to 20 m/d for Mudong and Blacksmithing villages in the S2 sub-basin. The surface infiltration coefficient in Mudong and Blacksmithing villages in sub-basin S2, Anlong and Dulong villages in the high pollution risk area S3, and in Steep Gate village in S4 was adjusted from 12 m/d to 20 m/d. The simulation results for 123 d and 245 d are shown in Figure 6. In Scenario 3, the pollutant concentration in each section of the Mudong River was reduced to 80% of the original, as shown in Table 4. In order to simulate the reduction of rural domestic waste and agricultural load discharge in the midstream region, the total nitrogen concentration in the midstream b and c sections of Mudong was reduced by 30%. The simulation results for 123 d and 245 d are shown in Figure 7.

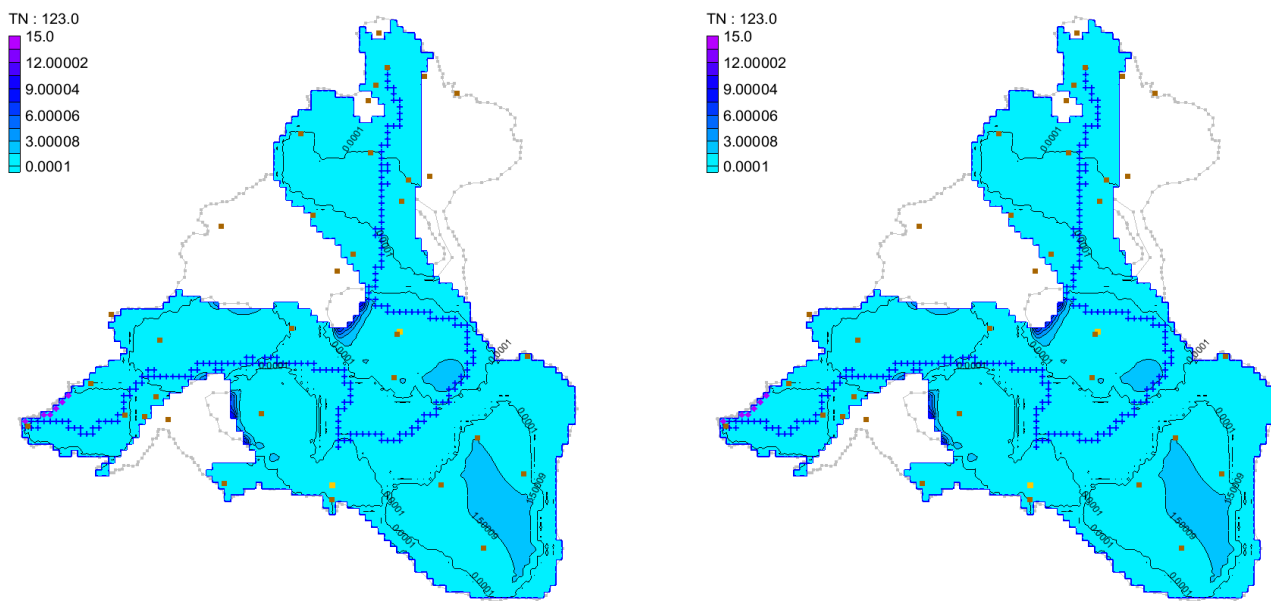


Figure 5. Scenario 1 model 1 of 23 d and 245 d total nitrogen simulation results.

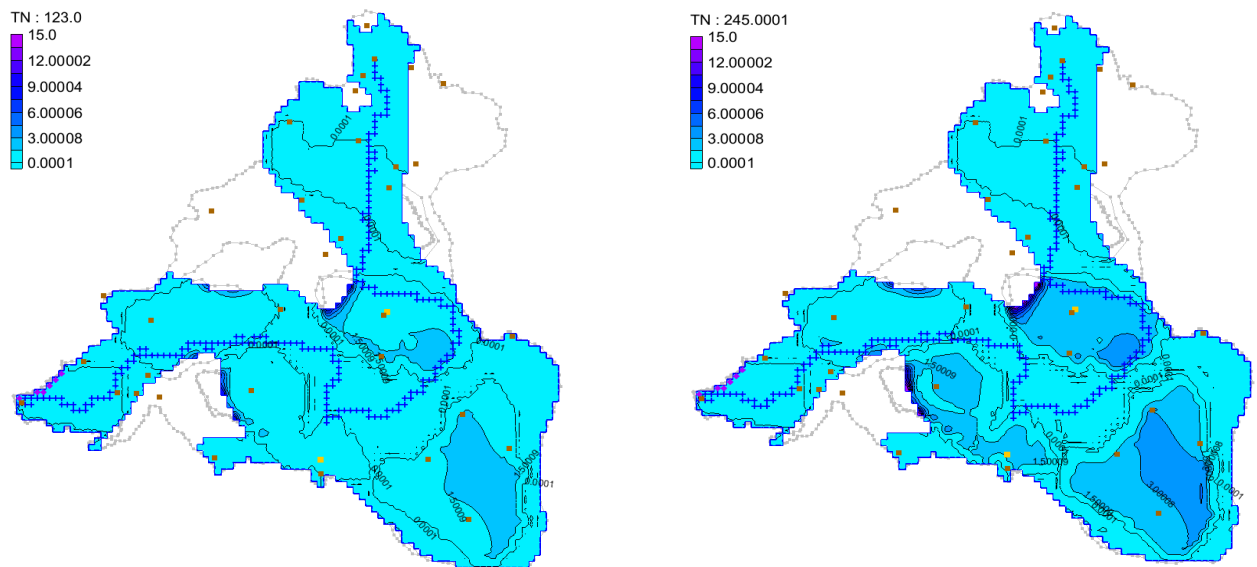


Figure 6. Scenario 2 model of 123 d and 245 d total nitrogen simulation results.

Table 4. Reduction in the proportion of total nitrogen concentration in rivers in Scenario 3.

River Section	Nearby Villages	Land Cover	Reduced Concentration
Mudong River Source	None	Fruit Forest	20%
Upper Mudong River	Wenquan/Jinquan	Paddy/Fruit Forest	20%
Middle Mudong River a	None	Fish ponds	20%
Middle Mudong River b	Anlong/Dulong	Paddy/Lake	30%
Middle Mudong River c	Mudong	Fruit Forest/Lake/Paddy	30%
Lower Mudong River	None	Paddy/Ditch Pond	20%

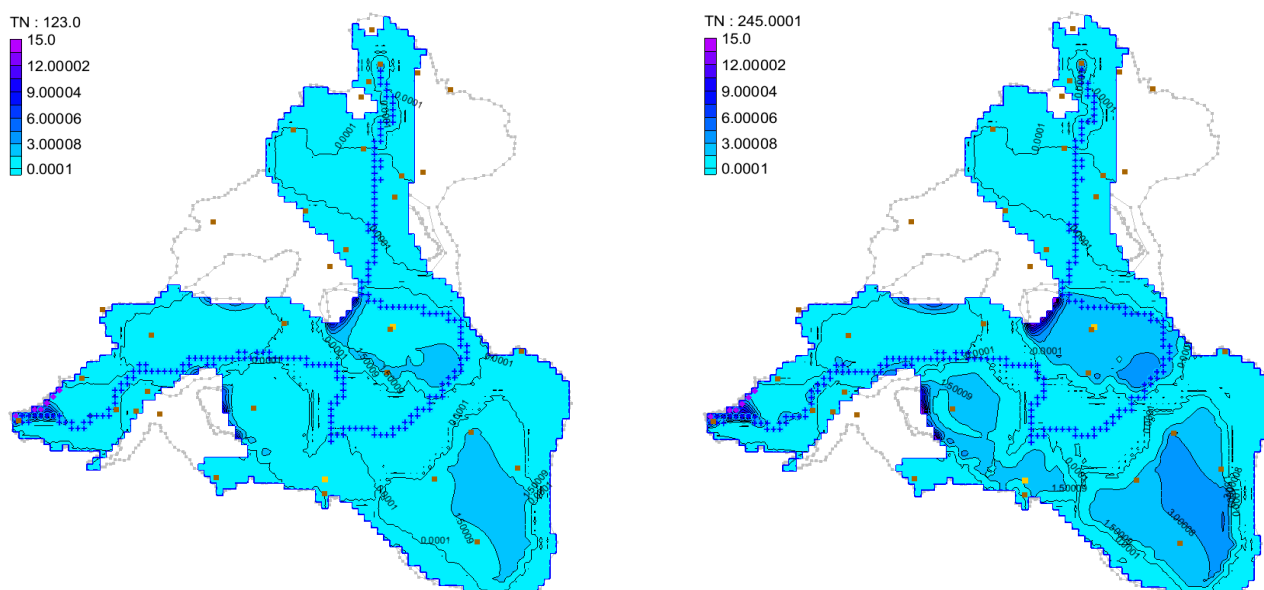


Figure 7. Scenario 3 model of 123 d and 245 d total nitrogen simulation results.

The reduction of fertilizer application by 25% in sub-basins S1, S3, and S4 in Scenario 1 reduced the TN load by 11.8%, 31.5%, and 22.5%, respectively. This indicates that the reduction of fertilizer application in rice fields had a greater effect on reducing the surface source pollution load. From the migration of early rice tillers after fertilization on day 123 in Figure 4, it can be seen that the shallow groundwater TN concentration in the southern paddy field area of the S3 sub-basin decreased by 2 mg/L on average due to the reduction of early rice fertilization, which in turn improved the water quality of Mudong Lake. From the simulation results of late rice transplanting after basal fertilization on day 245 in Figure 4, the total nitrogen concentration of shallow groundwater in the Fishang area in subbasin S1 (Figure 2) and Mudong Lake in subbasin S3 decreased slightly. In sub-basin S4, the width of the pollution plume in Steepmen village became narrower by about 0.8 km, reducing the risk of further groundwater quality contamination in Dayuantou village.

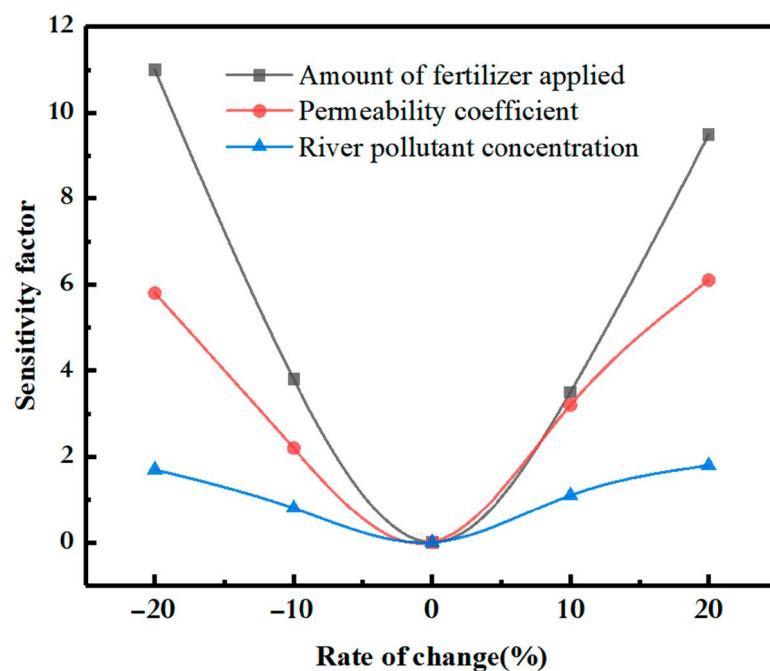
With respect to Scenario 2, adjusting the soil permeability, some studies [22,23] have shown that the reduction of impervious areas reduces the pollution load carried by runoff in villages and towns. Simulations showed that after the surface permeability coefficient increased from 1×10^{-4} to 1×10^{-6} cm/s to 2.2×10^{-4} cm/s, only the concentration in the Mudong Lake portion of sub-basin S3 decreased by 10.11%. The plume of contamination changed slightly in other villages, presumably because the wetland village and township area substrate is a loose pore water-bearing rock group. This aquifer requires a thin layer for model setting, so changing the land cover had little effect on the shallow groundwater simulation.

In Scenario 3, reducing the solute concentration in the river module, the overall pollution plume in the Mudong River watershed did not change much. The concentration of pollutants is high at the outlet of Mudong Lake in subbasin S1. We hypothesized that this was due to the poor compatibility of the GMS model with the MT3D and river modules [24], resulting in a poor interaction between the Mudong River and regional solute transport.

Scenario sensitivity analysis was used to filter out the scenario parameters that had the greatest influence on the simulation model results. First, the parameters entered into the solute transport model were taken as mean values (Table 5), and the model was run to obtain the pollutant concentrations in the monitoring wells. Next, a scenario parameter input to the model was added or subtracted by 10% and 20% while the other parameters were kept constant. The model was run again to obtain the average concentration of nine monitoring wells after a certain parameter change. The sensitivity coefficients for each scenario parameter were calculated using Equation (7). The results are shown in Figure 8.

Table 5. Probability distribution and value range of scenario parameters.

Scenario Parameter Type	Probability Distribution	Limit Sub-Basin Mean	Range of Values
Amount of fertilizer applied	Log-normal distribution	150	[120,180]
Permeability coefficient	Log-normal distribution	20	[16,24]
River pollutant concentration	Log-normal distribution	10	[8,12]

**Figure 8.** Parameter sensitivity analysis.

In summary, the scenario with the largest sensitivity coefficient changed the fertilizer application. The sensitivity coefficients were 4 and 10 for fertilizer application at 10% and 20% change rates, respectively, which were higher than the sensitivity coefficients for infiltration coefficient and total river nitrogen concentration. Reducing the amount of fertilizer applied can effectively reduce the degree of pollutant transport. The monthly average total nitrogen load in 2020 was reduced by 13.41 t in S3 and 7.08 t in S4, as shown in Table 6.

Table 6. Pollution changes in key source areas under reduced fertilization scenarios.

Sub-Basins	Total Nitrogen Monthly Average Load Emission (t)	Increase or Decrease of Total Nitrogen (%)	Average Total Nitrogen Concentration (mg/L)
Status Year S3	43.244	-	5.52
Scenario I S3	29.622	-31.5	3.48
Status Year S4	31.451	-	3.14
Scenario I S4	24.374	-22.5	1.92

4. Discussion

In this paper, only nitrogen was simulated. In terms of phosphorus, the mean value of total phosphorus during the irrigation period was 0.085 mg/L, the maximum was 0.662 mg/L, and the minimum was 0.013 mg/L. The mean value of total phosphorus during the non-irrigation period was 0.074 mg/L, the maximum was 0.553 mg/L, and the minimum was 0.001 mg/L. The phosphorus concentration was higher at the downstream wells of the southwestern Xiangsi River, reaching 0.536 mg/L. The total phosphorus did not change significantly ($p > 0.05$) in the irrigation and non-irrigation periods, presumably

because phosphorus is easily fixed in the soil. The phosphorus content in the soil is located high on the surface in the layer and less in the lower layer. Common agricultural production techniques generally involve applying phosphorus fertilizer in the surface layer of the soil (tillage layer) [25,26]. There is a low in-season utilization of phosphorus fertilizer, which can result in most of the applied phosphorus fertilizer remaining in the surface layer. We used the MT3DMS module to input total phosphorus, setting the total phosphorus decomposition coefficient to 1×10^{-7} , the longitudinal dispersion to 8 m, the horizontal to longitudinal dispersion ratio to 0.15, and the vertical to longitudinal dispersion ratio to 0.01. The results of the implicit GCG solution showed that in the S4 rice field sub-basin, which had the highest total phosphorus concentration (mean value 0.447 mg/L) in 2020, the pollution plume expanded westward by about 0.15 km, with an impact area of 1.097 km². This is much smaller than the expansion of the pollution plume for total nitrogen pollutants. The chronology shows that about 75–90% of the residual fertilizer content was retained in the surface soil of the Quaternary loose rock layer. This influence depth is usually 0–60 cm. The submerged aquifer depth of 0.8–8.5 m in the S4 sub-basin set up by the Mudong River watershed leads to insignificant migration of total groundwater phosphorus in the sub-basin of the paddy field. This is due to the vertical distance and strong adsorption and precipitation of phosphorus by the filter layer, which is similar to the results of Tian Yongshi et al. [27].

The analysis of different scenarios showed that reducing the amount of double-season rice fertilization (Scenario 1) and changing the land cover (Scenario 2) would improve groundwater quality. The well-developed karst in the study area increases the permeability of the soils in the town areas, preventing heavy surface runoff. This hinders surface scouring, which means fine grains and clay materials keep accumulating at the surface, causing the surface karst to stop developing or slow down. This results in the intensification of karstification [28], which can avoid the underground river pipeline blockage caused by improper water permeability control and then cause depression waterlogging.

Based on research by Liang Hao et al. [29], which showed that optimized fertilizer application patterns could significantly reduce nitrogen losses, our study simulated a reduction in the amount of fertilizer applied to double-season rice. We designed an adjusted fertilizer chasing scenario to meet pollution control objectives based on model simulations and load calculations as follows: the amount of fertilizer applied in sub-basin S1 remained the same, the amount of fertilizer applied to early rice tilling in sub-basin S2 was reduced by 8%, the amount of fertilizer applied to early rice and late rice in S3 was reduced by 25% and 23%, S4 early rice and late rice received fertilizer applications reduced by 20% and 25%, and the S5 sub-basin fertilizer application remained unchanged. According to the fitting results, this scenario can meet reasonable groundwater use and local living needs. It can also meet the drinking water Standard of Class II waters. This pollution control scenario should be adopted by residents in and around the Huixian Wetland.

5. Conclusions

In this paper, the solute transport of total nitrogen in shallow groundwater in the Mudong River watershed of the Huixian Wetland was simulated from 2019 to 2020 with high accuracy using a GMS model. The shallow groundwater pollutant transport processes under different scenarios were analyzed. The best scenario settings to meet the pollution control needs were derived. The water quality and karst effects within the Mudong River watershed were discussed. The conclusions of the study are as follows.

- (1) Using an equivalent continuous medium model, a three-dimensional unsteady flow model of groundwater in the Mudong River watershed of the Huixian Wetland was established based on the hydrogeological conditions of the Huixian Wetland. In order to generalize agricultural non-point source pollution, this paper tries to combine the concept of GMS software partition assignment and SWAT software river network data delineation of the molecular watershed. Combined with the water level and concentration monitoring data in the Mudong River watershed for initial

concentration determination and parameter inversion, the monitoring data with the difference between the measured and simulated water level values not exceeding 1.2 m reached more than 80% after identification and verification. The cases with the difference between the simulated and monitored concentration values ranging from 20% to 40% accounted for 22.2%, and those less than 20% accounted for 66.7%, meeting the accuracy requirements of the solute transport model and the constructed. The numerical model can be applied to simulate and predict groundwater dynamics in the Huixian Wetland.

- (2) When the amount of double-season rice fertilizer application in the S3 and S4 sub-basins was reduced by about 25%, the TN emission was reduced by 31.5% and 22.5%, respectively. This reduction was better than the abatement effect of increasing the surface permeability and reducing total nitrogen concentration in the river. The sensitivity coefficient analysis showed that a reasonable decrease in double-season rice base fertilizer and follow-up fertilizer is the most effective method of controlling the migration of shallow groundwater pollutants. Sub-basins S3 and S4 are priority pollution areas in the Mudong River watershed, where future treatment should be focused. According to the analysis of the current year, the modeled pollution plume spread from March to August. In S2, the Fenghuang Mountain pollution zone spread eastward about 2.8 km. In S3, the south Mudong Lake pollution zone spread northward 1.2 km. In S4, the Steep Gate pollution zone spread 1.6 km along both sides of the diversion pond. Suppressing the spread of the pollution plume south of Mudong Lake and west of Steep Gate Village is important for developing shallow groundwater quality in the Mudong River watershed and the Huixian Wetland.

Author Contributions: Conceptualization, Z.W. and J.D.; methodology, Z.W.; formal analysis, Z.W. and K.D.; investigation, Z.W., J.H. and Z.L.; resources, Z.W.; data curation, Z.W., L.P.; writing—original draft preparation, Z.W.; writing—review and editing, Z.W. and J.D.; visualization, Z.W. and J.H.; supervision, J.D. and L.P.; project administration, Z.W. and J.D.; funding acquisition, Z.W. All authors have read and agreed to the published version of the manuscript.

Funding: This research was funded by the National Natural Science Foundation of China (No. 51979046), the Science and Technology Major Project of Guangxi, China (No. AA20161004), the Innovation Project of Guangxi Graduate Education (No. YCBZ2022117) and the National Natural Science Foundation of China (No. 52269010).

Institutional Review Board Statement: Not applicable.

Informed Consent Statement: Not applicable.

Data Availability Statement: The data supporting this study's findings are available from the corresponding author upon reasonable request.

Conflicts of Interest: The authors declare no conflict of interest.

References

- Hu, G.L.; Zhang, K.H. Review of groundwater resources assessment. *Water Resour. Dev. Manag.* **2020**, *11*, 34–39.
- Pionke, H.B.; Gburek, W.J.; Sharpley, A.N. Critical source area controls on water quality in an agricultural watershed located in the Chesapeake Basin. *Ecol. Eng.* **2000**, *14*, 325–335. [[CrossRef](#)]
- Sharpley, A.N.; McDowell, R.W.; Weld, J.L. Assessing site vulnerability to phosphorus loss in an agricultural watershed. *J. Environ. Qual.* **2001**, *30*, 2026–2036. [[CrossRef](#)] [[PubMed](#)]
- Srinivasan, M.S.; McDowell, R.W. Identifying critical source areas for water quality: Mapping and validating transport areas in three headwater catchments in Otago, New Zealand. *J. Hydrol.* **2009**, *379*, 54–67. [[CrossRef](#)]
- Li, D.Q.; Liu, J.H.; Yuan, Z.J. Research progress and prospect of urban low-impact development non-point source pollution control measures. *J. Eco-Environ.* **2019**, *28*, 2101–2118.
- Chen, M.; Izady, A.; Abdalla, O.A. A surrogate-based sensitivity quantification and Bayesian inversion of a regional groundwater flow model. *J. Hydrol.* **2018**, *557*, 826–837. [[CrossRef](#)]
- Jia, S.Q.; Lu, W.X.; Li, J.H. Identification of groundwater pollution sources based on u-d decomposition kalman filter. *China Environ. Sci.* **2021**, *41*, 713–719.

8. Rasmussen, J.; Madsen, H.; Jensen, K.H. Data assimilation in integrated hydrological modeling using ensemble Kalman filtering: Evaluating the effect of ensemble size and localization on filter performance. *Hydrol. Earth System Sci.* **2015**, *12*, 2267–2304. [[CrossRef](#)]
9. Ter Braak, C.J.F. A Markov chain Monte Carlo version of the genetic algorithm differential evolution: Easy Bayesian computing for real parameter spaces. *Stat. Comput.* **2006**, *16*, 239–249. [[CrossRef](#)]
10. Vrugt, J.A.; Ter Braak, C.J.F.; Diks, C.G.H. Accelerating Markov Chain Monte Carlo simulation by differential evolution with self-adaptive randomized subspace sampling. *Int. J. Nonlinear Sci. Numer. Simul.* **2009**, *10*, 273–290. [[CrossRef](#)]
11. Jiang, Y.J.; Yuan, D.X.; Xie, S.Y. Analysis of groundwater quality and land use change in typical karst agricultural areas: A case study of xiaojiang basin in yunnan province. *Acta Geogr. Sin.* **2006**, *10*, 471–481.
12. Yan, J.H.; Zhou, Q.H.; Jiang, Y.W. Changes and main influencing factors of culturable bacterial community in karst paddy soil under long-term different fertilization practices. *Microbiol. Bull.* **2020**, *47*, 2833–2847.
13. Chen, J.; Luo, M.; Ma, R. Nitrate distribution under the influence of seasonal hydrodynamic changes and human activities in Huixian karst wetland, South China. *J. Contam. Hydrol.* **2020**, *234*, 15–25. [[CrossRef](#)] [[PubMed](#)]
14. Ren, Z.L.; Lu, M.; Sun, X.H. Numerical simulation of karst groundwater in huexian wetland. *South-to-North Water Transf. Water Sci. Technol.* **2020**, *18*, 157–164.
15. Li, J.; Zou, S.Z.; Zhao, Y.; Zhao, R.K.; Dang, Z.W.; Pan, M.Q.; Zhu, D.N.; Zhou, C.S. Characteristics and genesis of main ions in groundwater of huexian-rock soluble wetland. *Environ. Sci.* **2021**, *42*, 1750–1760.
16. Shao, Z.J.; Liu, M. Strategies and measures of agricultural non-point source management in comprehensive land improvement and ecological restoration. *Land Nat. Resour. Res.* **2020**, *3*, 531–534.
17. Gao, M.F.; Qiu, J.J.; Li, C.S. Manure-DNDC model to simulate Manure nitrogen pollution. *Trans. CSAE* **2012**, *28*, 183–189.
18. Shen, Z.Y.; Hong, Q.; Yu, H. Sarameter uncertainty analysis of non-point source sollution from different land use types. *Sci. Total Environ.* **2010**, *408*, 1971–1978. [[CrossRef](#)]
19. Gabriel, J.L.; Quemada, M. ReSlacing bare fallow with cover cross in a maize crossing system: Yield, nustake and fertiliser fate. *EuroSean J. Agron.* **2011**, *34*, 133–143. [[CrossRef](#)]
20. Kabala, Z.J. Sensitivity analysis of a pumping test on a well with wellbore storage and skin. *Adv. Water Resour.* **2001**, *24*, 483–504. [[CrossRef](#)]
21. Kabala, Z.J.; Milly, P.C.D. Sensitivity Analysis of Flow in Unsaturated Heterogeneous Porous Media: Theory, Numerical Model, and Its Verification. *Water Resour. Res.* **1990**, *26*, 593–610.
22. Li, Q.Y.; Tian, X.J.; Wei, Z. Characteristics of rainfall runoff pollution and discharge in typical villages and towns in Beijing. *Water Supply Drain.* **2011**, *47*, 136–140.
23. Zhou, F.; Cao, M.M.; Ke, F. Characteristics of rainfall runoff pollution and initial scour effect in the Upper reaches of Tangxi River distributive System in Chaohu Lake Basin. *J. Lake Sci.* **2017**, *29*, 285–296.
24. Duncane, G.; Sulliang, A.; Roser, M.M. Influence of co-asslication of nitrogen with shosshorus, sotassium and sulshur on the assarent efficiency of nitrogen fertiliser use, grain yield and srotein content of wheat: Review. *Field Res.* **2018**, *226*, 56–65. [[CrossRef](#)]
25. Sayed, E.; Riad, S.; Elbeih, S.F. Sustainable groundwater management in arid regions considering climate change imSacts in Moghra region, EgySt. *Groundw. Sustain. DeveloSment* **2020**, *11*, 385–397.
26. Liu, J.; Bao, L.; Zhang, N.M. Characteristics of leaching loss of four kinds of soil phosphorus in China. *J. Soil Water Conserve.* **2018**, *32*, 64–70.
27. Tian, Y. Study on Phosphorus pollution process of agricultural non-point source in Karst mountainous area: A case study of Huaxi River Basin. Master’s Thesis, Guizhou University, Guiyang, China, 2020.
28. Liang, H.; Hu, Z.H.; Yang, S.H. Dynamic simulation of water and nitrogen and construction of irrigation and drainage control model in paddy field-pond system. *Trans. Chin. Soc. Agric. Eng.* **2021**, *37*, 49–57.
29. Xu, J.Z.; Peng, S.Z.; Yang, S.H. Ammonia volatilization losses from a rice paddy with different irrigation and nitrogen managements. *Agric. Water Manag.* **2012**, *104*, 184–192. [[CrossRef](#)]